Available online at www.sciencedirect.com
SCIENCE DIRECT®
Polymer 45 (2004) 1185–1195
polymer
www.elsevier.com/locate/polymer

Synthesis of reactive hyperbranched and star-like polyethers and their use for toughening of vinylester–urethane hybrid resins

J. Karger-Kocsis[a,*], J. Fröhlich[b], O. Gryshchuk[a], H. Kautz[b], H. Frey[c], R. Mülhaupt[b]

[a]*Institut für Verbundwerkstoffe GmbH, Technische Universität Kaiserslautern, P.O. Box 3049, D-67653 Kaiserslautern, Germany*
[b]*Institut für Makromolekulare Chemie, Albert-Ludwigs-Universität Freiburg, Stefan-Meier-St. 31, D-79104 Freiburg, Germany*
[c]*Institut für Organische Chemie, Johannes-Gutenberg-Universität Mainz, Duesbergweg 10-14, D-55128 Mainz, Germany*

Received 13 June 2003; received in revised form 20 October 2003; accepted 8 December 2003

Abstract

A vinylester–urethane hybrid resin (VEUH) was toughened by adding various vinyl-functionalized branched polyethers in 10 and 20 wt%. Two sets of hyperbranched polymers (HBPs) with different branching density were compared with a set of six-arm star polymers. Besides the architecture, the polymers also varied in their characteristics (molecular mass and mass distribution, vinyl/hydroxy ratio). The morphology of the modified VEUH was studied by dynamic-mechanical thermal analysis (DMTA), transmission (TEM) and scanning electron microscopy (SEM). The toughness was characterized by the fracture energy (G_c) determined on compact tension specimens at room temperature. It was established that the architecture and vinyl/hydroxy ratio of the HBPs are those parameters which control the morphology and thus the related linear elastic fracture mechanical response. Less compact star-like polymers with long, flexible arms and with high vinyl functionality produced the largest toughness improvement in VEUH.

Keywords: Fracture mechanics; Hyperbranched polyether; Vinylester resin

1. Introduction

The discovery of dendritic and hyperbranched polymers [1] triggered vigorous interest for their potential application in both thermoplastic and thermoset resins [2–7]. It was reported that functional hyperbranched polymers (HBP) may be useful toughening for thermosetting resins, such as unsaturated polyesters [5], vinylesters (VE) [5,8] and epoxies [6,7,9]. Improved toughness is due to local inhomogeneties in the crosslinked network caused by the covalent incorporation of HBP molecules. It is intuitive that only a fraction of the functional groups in the shell of the HBP participate in the related crosslinking reaction. Accordingly, a very regular and thus 'compact' functional HBP is less effective modifier than a less compact one, since the functional groups of the latter are more accessible during the co-crosslinking procedure. Thus, a straightforward strategy is to tailor both the architecture and functionality of the HBP with respect to the thermosetting resin to be modified. In our earlier paper, commercially available epoxy and vinyl functionalized hyperbranched polyesters were used to modify a vinylester–urethane hybrid resin (VEUH) [8]. Recall that the crosslinking of VEUH occurs both via copolymerization with styrene (St) and polyaddition between the secondary OH groups of the VE and the NCO groups of the polyisocyanate added [10,11]. Aims of the current work are the application of branched polyethers with both vinyl and hydroxy functionalities as toughening modifiers for a VEUH resin. Two sets of HBPs are compared with a set of six-arm star polymers. The characterization of their efficiency is related to the architecture and the vinyl/hydroxy ratio. Note that the selected polymers bear vinyl as well as hydroxy groups which are involved in both copolymerization and polyaddition reactions during the curing of VEUH. The interest for polyether-based hyperbranched polymers is due to the expectation that they are more stable to hydrolysis than the polyester counterparts.

* Corresponding author. Tel.: +49-631-2017203; fax: +49-631-2017198.
E-mail address: karger@ivw.uni-kl.de (J. Karger-Kocsis).

0032-3861/$ - see front matter © 2003 Elsevier Ltd. All rights reserved.
doi:10.1016/j.polymer.2003.12.050

2. Experimental

2.1. Materials

The VEUH resin contained a bisphenol-A based styrene-diluted VE of the bismethacryloxy type (Daron® XP-45-A-2) and novolac-based polymeric isocyanate (Daron® XP 40-B-1), both products of DSM Composite Resins (The Netherlands). For its curing 1.5 phr peroxide (dibenzoylperoxide, Lucidol®CH-50L of Akzo Nobel, Germany; peroxide content: 50 wt%) and 1.5 phr accelerator (*N*,*N*-diethylaniline, NL-64-10P, Akzo Nobel; active component: 10 wt%) were used.

2.2. Preparation of the HBPs

The basic synthesis route of the hyperbranched polyethers, viz. ring opening multibranching polymerization of glycidol, was disclosed earlier [12–15]. For this study, glycidol was polymerized on a commercially available six-arm star poly(propylene oxide) end-tipped with ethylene oxide (Baygal VP.PU 99IK01 P.64, molar mass of 3300 g/mol from Bayer AG, Germany). The initiator/monomer ratio was chosen according to the desired molecular weight of 5000 g/mol for the product. Two propylene oxide units were directly polymerized onto each polyglycerol chain end in a following reaction step. Functionalization was achieved by subsequent polymerization of allyl glycidyl ether (AGE). Two hyperbranched radial block copolymers consisting of a poly(propylene oxide) core, a polyglycerol and a poly(propylene oxide) but different poly(allyl glycidyl ether) shells were obtained as transparent, viscous liquids after protonation with ion exchange resin in methanol and removal of the solvents.

A second set of HBPs was prepared similarly to the first. In this case, however, the glycidol was statistically copolymerized with AGE onto the poly(propylene oxide) core. Additional functionalities were introduced into the polymer shell by subsequent polymerization of AGE alone. Two radial block copolymers consisting of a poly(propylene oxide) core, a poly(glycerol-*co*-allyl glycidyl ether) layer and two different poly(allyl glycidyl ether) shells were obtained as transparent, viscous liquids.

To prepare a set of six-arm star polymers for comparison, AGE was anionically polymerized onto a six-arm star poly(propylene oxide) core (Baygal VP.PU 99IK01 P.65, molar mass of 12,000 g/mol from Bayer AG, Germany) by slow monomer addition. Two star block copolymers consisting of a poly(propylene oxide) core and two different poly(allyl glycidyl ether) shells were obtained as transparent, viscous liquids.

Polymer analysis by means of ^{1}H and ^{13}C NMR spectroscopy as well as size exclusion chromatography (SEC) and dynamic scanning calorimetry (DSC) was conducted as reported elsewhere [12]. Based on the molecular parameters of the polymers (cf. Table 1), the toughness performance of the modified VEUH can be traced back to effects of architecture, functionality and relative functionality (i.e. vinyl/hydroxy) as well as molecular weight.

2.3. Specimen preparation

The branched polyethers with hydroxy and vinyl functionalities were added to the resin as modifiers in amounts of 10 and 20 wt%, respectively. Compact-tension (CT) specimens were produced by pouring the homogenized and degassed resin mixture in steel molds possessing a bolted cover plate for easy demolding of the specimens. Curing of all resin mixtures was carried out under the following conditions: mixing, homogenization, degassing and filling of the mold occurred at ambient temperature, then the temperature was raised to 50 °C for 15 min, 80 °C for 30 min, 140 °C for 30 min, and finally 200 °C for 60 min.

2.4. Materials testing

The phase structure of the toughened VEUHs was characterized by dynamic mechanical thermal analysis (DMTA). DMTA spectra were taken on rectangular specimens ($50 \times 10 \times 4$ mm^3; length × width × thickness) in flexural mode at 10 Hz using a Eplexor 25N device of Gabo Qualimeter. The static and cyclic (sinusoidal) loading components were set to 10N and ± 5N, respectively. DMTA spectra, viz. complex modulus (E^*) and its constituents (E' and E''), mechanical loss factor (tan δ) as a function of temperature (T), were measured in the interval $T = 0$ to +300 °C at a heating rate of 1 °C/min.

Transmission electron microscopic (TEM) investigations were carried out with a Leocem 912 Omega device applying an acceleration voltage of 120 kV. The specimens were prepared using an Ultracut (Reichert and Jung) ultramicrotome. Thin sections of about 50 nm were produced with a Diatome diamond knife at room temperature. The samples were stained with RuO_4.

Fracture energy (G_c) was determined on the CT specimens in accordance with the ESIS testing protocol [16]. The CT specimens (dimension: $35 \times 35 \times 4$ mm^3) were notched by sawing. Their notch root was sharpened by a razor blade prior to their tensile loading (mode I) at room temperature on a Zwick 1445 machine with a crosshead speed of $v = 1$ mm/min.

In order to get a deeper understanding on the effect of morphology on the fracture mechanical response, the surfaces of the broken CT specimens were inspected in a scanning electron microscope (SEM; JSM-5400 of Jeol). Each fracture surface was coated with an alloy of Au/Pd prior to SEM investigations.

Table 1
Molecular characteristics of the functional branched polyethers used. Molecular weight, number of incorporated comonomers (n) and polymer functionalities (f) were calculated from NMR; T_g was elucidated from DSC

	M_n (g/mol)	n(Gly)	f(OH)	n(AGE)	f(C=C)	f(C=C)/f(OH)	T_g (°C)
25V10	10,500	27	33	25	25	0.76	−62
84V15	15,400	27	33	84	84	2.55	−70
75V17	16,900	63	68	75	75	1.10	−67
83V18	18,200	73	79	83	83	1.05	−78
23V15	14,600	0	6	23	23	3.83	−68
50V18	17,800	0	6	50	50	8.33	−73

3. Results and discussion

3.1. Polymer synthesis

Three different sets of hyperbranched polymers (HBPs) of various architecture were involved in this study. For the first set, HBPs were polymerized from glycidol with a six-arm star poly(propylene oxide) as core molecule using the slow monomer addition technique to yield polyglycerol (PGly). In order to reduce the high polarity of the polyglycerol, propylene oxide (PO) was directly polymerized onto the living polyglycerol chain ends without altering the total number of hydroxy end groups [13]. This reaction step yielded the hyperbranched block copolymer PGlyPO. Subsequently, allyl glycidyl ether (AGE) was polymerized onto the living chain ends to introduce C=C functionalities. Thus, two multilayered block copolymers consisting of the same core of poly(propylene oxide)-*block*-(ethylene oxide) with a hyperbranched layer of polyglycerol and a layer of poly(propylene oxide) were obtained. They differed, however, in the composition of their poly(allyl glycidyl ether) shells bearing numerous allyl and secondary hydroxy groups (cf. Scheme 1) and were designated 25V10 and 84V15, respectively. The designation used for all polymers in this study indicates the vinyl (V) functionality by the first digits and the number-average molecular weight (more exactly M_n/1000) by the last two digits. The polymers were analyzed during the stepwise polymerization procedure by means of ^{1}H and ^{13}C NMR as well as SEC. NMR reveals the exact compositions of the branched polymers. From the number of monomer units present in each polymer (designated n(Gly) and n(AGE) in Table 1 for glycidol and AGE, respectively), the molecular weight M_n could be calculated. Fig. 1 shows the four ^{1}H NMR spectra taken during the polymerization procedure. Starting from polyglycerol, one can observe the additional peaks resulting from the copolymerization of first PO (alkyl protons at 1.2 ppm and ether protons at 4.1 ppm) and secondly AGE in different amounts (allyl protons at 5.2 and 5.8 ppm as well as additional ether protons at 4.2 ppm). SEC clearly proved molar mass increase throughout the polymerization procedure, while polydispersity stayed on a very low level with $M_w/M_n < 1.6$. Furthermore, the apparent molecular masses, recorded by SEC, closely match both calculated and NMR-derived values (cf. Table 2).

The second set of HBPs was prepared similar to the first set. To reduce the branching density of these polymers, glycidol and AGE were statistically copolymerized onto the

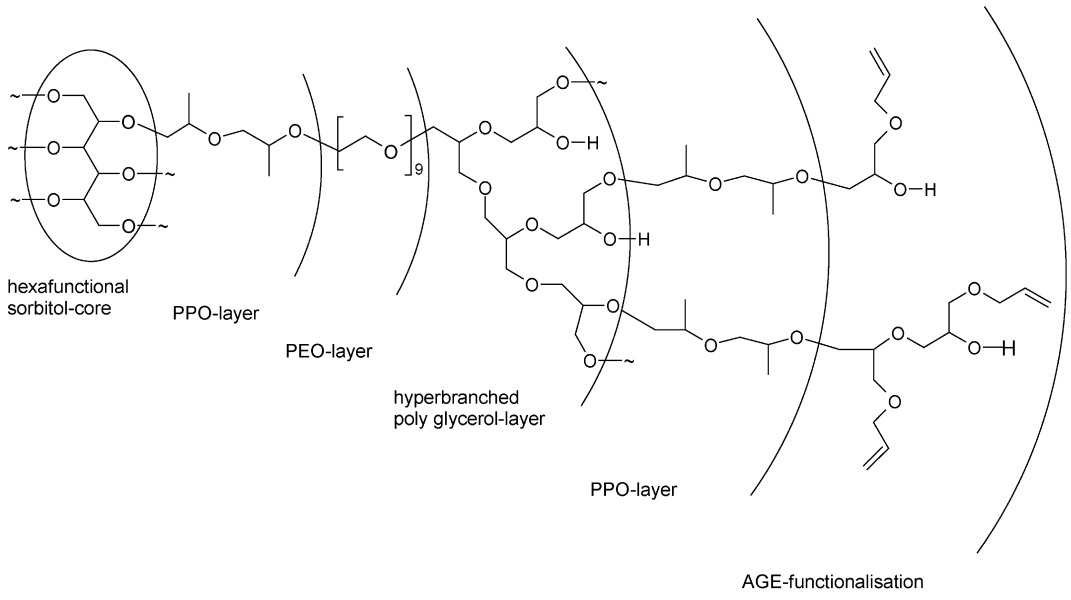

Scheme 1. Multilayered structure of the first set of HBPs (25V10 and 84V15).

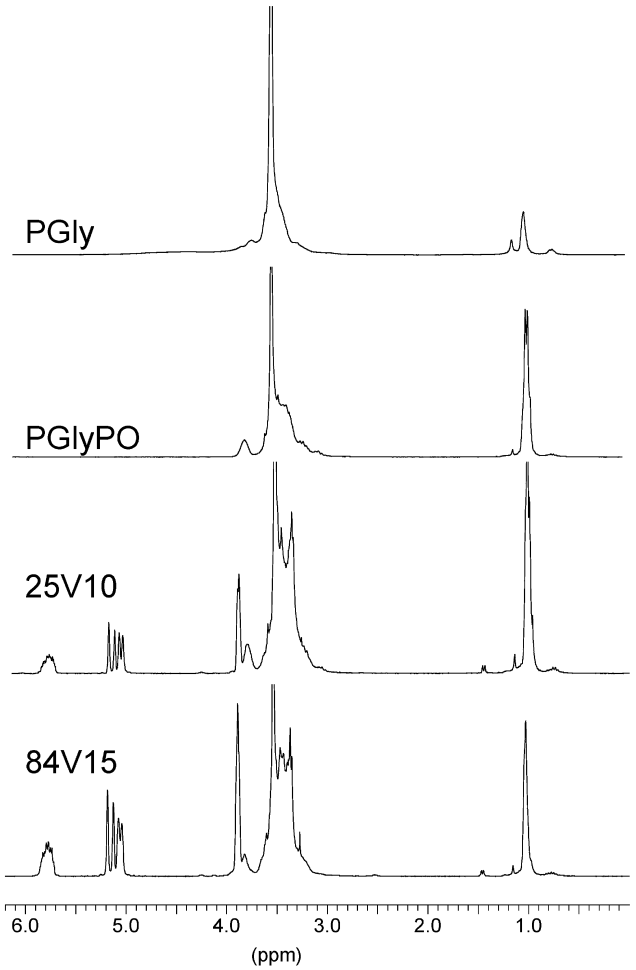

Fig. 1. ^{1}H NMR spectra of hyperbranched block copolymers taken during stepwise build-up of the multilayer architecture.

same hexavalent core [15]. These polymers were functionalized in the outer shell by the subsequent homopolymerization of AGE similarly to the first set. Finally, two multilayered block copolymers consisting of a core of poly(propylene oxide)-*block*-(ethylene oxide), a hyperbranched layer of poly(glycerol-*co*-allyl glycidyl ether) and two different shells of poly(allyl glycidyl ether) bearing allyl and secondary hydroxy groups were obtained (75V17 and 83V18 shown in Scheme 2).

A set of six-arm star polymers was prepared for comparison with the HBPs. AGE was polymerized with a six-arm star poly(propylene oxide) as core molecule (12,000 g/mol) by slow monomer addition. Two star block copolymers consisting of a poly(propylene oxide) core and two different poly(allyl glycidyl ether) blocks bearing numerous C=C functionalities were obtained (23V15 and 50V18 displayed in Scheme 3). The molecular weights of the star polymers were comparable to those of the HBPs presented above. Because of the low number of hydroxy end groups of the six-arm star polymers, the vinyl/hydroxy ratios of these polymers are significantly higher than for the HBPs.

Table 2
Comparison between calculated and by SEC determined molecular mass values

	M_{calc} (g/mol)	M_w (g/mol)	M_n (g/mol)	M_w/M_n
PPO core	3270	3700	3300	1.1
PGly	5000	7100	5600	1.3
PGlyPO	8480	9500	6900	1.4
25V10	11,900	12,800	9000	1.4
84V15	18,740	19,900	12,500	1.6

The polymeric products of the second and third sets were also analyzed by means of NMR and SEC. The characteristics of all polymers are listed in Table 2. The molecular weights of the polymeric modifiers range between 10,000 and 18,000 g/mol. The polydispersities of all samples are considerably low.

The T_gs of the liquid polymers, measured by DSC, range between −60 °C and −80 °C whereas, the polymer with the higher amount of AGE possesses the lower T_g in a series with the same architecture (cf. Table 1). Thus, in spite of the growing molecular weight, the T_g is depressed because the polymers are rendered less polar. When the concentration of hydroxy end groups is lowered, the tendency to the formation of intermolecular hydrogen bonds is decreased. These interactions, however, usually govern the glass transition temperatures of hyperbranched polymers.

3.2. DMTA behavior

The incorporation of the various HBPs into the VEUH resin gave three different types of DMTA spectra. Type 1 showed a shift in the glass transition (T_g) toward lower temperatures and a decrease in the stiffness above room temperature with increasing HBP content (cf. Fig. 2). This response was observed for the modifiers 25V10, 75V17 and 83V18. Note that all of them have similar f(C=C)/f(OH) ratios of about 1.0 (cf. Table 1). The tan δ vs. T traces showed the appearance of a shoulder at $T \approx 70$ °C in presence of the related HBP. This relaxation is believed to reflect the presence of highly irregular network sections the formation of which is favored by the modifiers built-in [8, 11].

The second type of the DMTA spectra showed similar features as the first type except that the added HBP strongly reduced the stiffness over the whole temperature range measured. This response was found for the VEUH modified by 84V15 (cf. Fig. 3). Note that for this HBP the vinyl functionality is considerably higher than the hydroxy functionality (cf. Table 1).

The third type is similar to the second except that the relaxation peak referring to the T_g was shifted toward slightly higher temperatures and, at the same time, this relaxation became less pronounced. This behavior was found for the modifiers 23V15 and 50V18 (cf. Fig. 4). Recall that both of these macromolecules are six-arm star polymers and no 'true' HBPs. The hydroxy functionality is

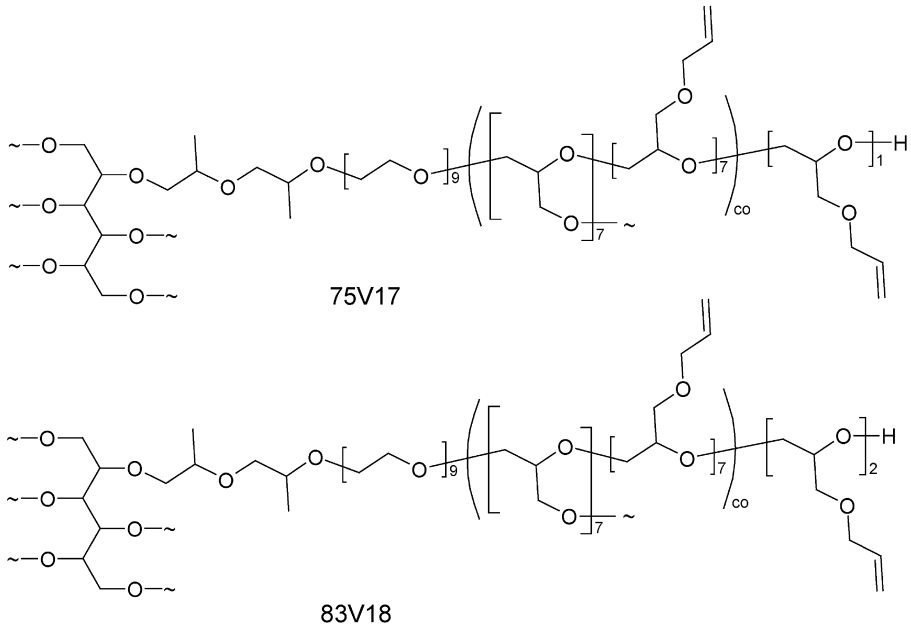

Scheme 2. Structure of HBPs 75V17 and 83V18.

negligible compared to the vinyl functionality (cf. Table 1). The type 3 DMTA response, shown in Fig. 4, is quite unique. A decrease in stiffness accompanied by a lowering of the T_g are usual effects of 'reactive diluents' in thermosets. This was also observed for the DMTA behavior of types 1 and 2 modifiers (cf. Figs. 2 and 3). On the other hand, decreased stiffness accompanied by T_g increment is unexpected and must have morphological reasons. In order to shed light on this issue the morphology of the systems was studied by TEM and SEM techniques.

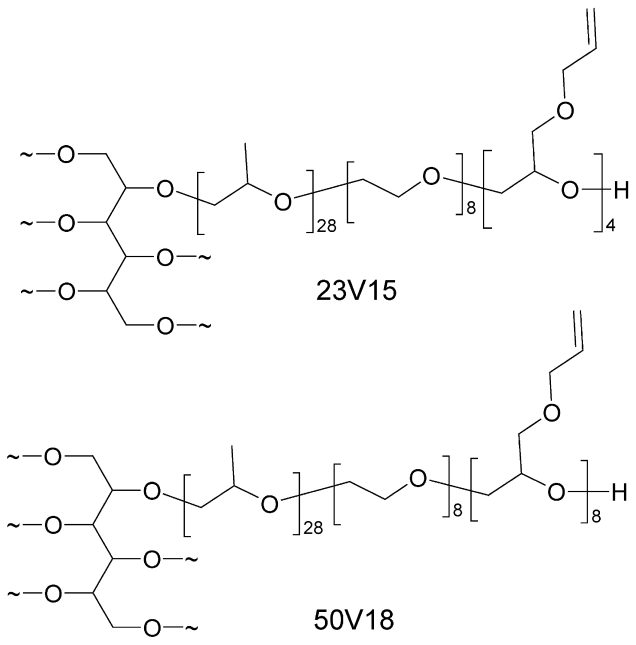

Scheme 3. Structure of HBPs 23V15 and 50V18.

3.3. Phase structure

Fig. 5 shows a TEM picture taken from the VEUH modified by 20 wt% 25V10. Recall that this modifier gave type 1 DMTA response. The bright large inclusions stem from the agglomeration of HBP molecules. Their presence could also be detected by SEM on the fracture surface of this VEUH system—cf. Fig. 6. The 'dendritic' feature (indicated by arrows in Fig. 6) of these inclusions suggests that they were likely formed by homopolymerization of the related HBPs via their C=C moieties (cf. Schemes 1–3). A prominent 'dendritic' structure is depicted in Fig. 7 in higher magnification. Based on the above findings, the type 1 DMTA response of the HBPs 25V10, 75V17 and 83V18 is likely linked to a complex phase structure containing HBP molecules built in the crosslinked network as well as phase-segregated homopolymerized HBP domains. Because the HBP molecules are only partly incorporated on a molecular basis in the matrix network and the homopolymerized fraction works like a filler, the stiffness of the related resins is only slightly affected.

TEM images of the modified VEUH of DMTA type 2 and 3 are quite similar. Fig. 8 shows an example of the morphology of VEUH containing 20 wt% 50V18. The structure in Fig. 8 resembles an interpenetrating network (IPN). However, IPN-structured thermosets generally exhibit a loss in both stiffness and T_g [17]. Note that the latter effect does not appear for type 3 modifiers (cf. Fig. 4) in the presence of which the T_g shifts toward higher temperatures. Recall that the HBPs may be involved via their vinyl functionalities in both homo- and copolymerization reactions. The latter extends also for copolymerization with VE and St. Parallel to that VE and St homo- and copolymerize (with each other), too. Further, the hydroxy

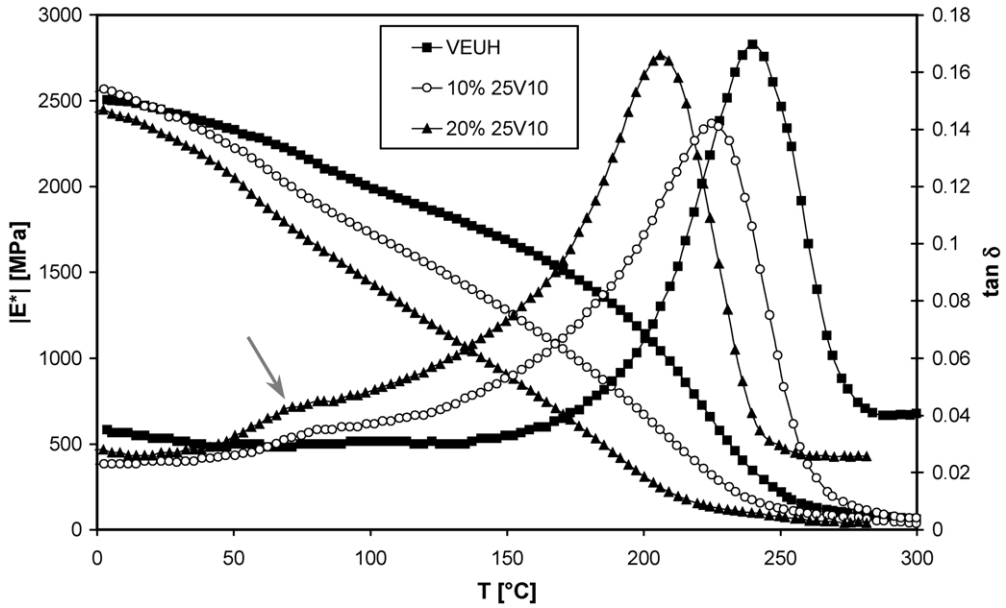

Fig. 2. $|E^*|$ vs. T and tan δ vs. T traces for VEUH without and with 10 and 20 wt% 25V10. Note: arrow indicates the additional relaxation transition.

functions of the HBP and VE react with the isocyanate groups of the polyisocyanate compound present in VEUH. The outcome is a very complex network structure containing more or less tightly crosslinked sections owing to the different reactions. In addition, the vinyl homo- (mostly) and copolymerization reactions may yield considerable phase-segregation characterized by inclusions of fine or coarse distributions. If copolymerization reactions dominate in the system then reduced stiffness and T_g can be predicted. The same note holds for the VEUH modification with HBPs of high hydroxy functionality. In this case the probability of polyaddition reactions between the isocyanate groups of the polyisocyanate and hydroxy groups of HBP is markedly higher than between polyisocyanate and secondary hydroxy groups of VE.

So, the difference between types 2 and 3 HBPs is apparently related to the hydroxy functionality. When the hydroxy functionality is quite high (cf. 85V15 as DMTA type 2), a less crosslinked structure by vinyl polymerization develops as the isocyanate compounds also reacts with the OH groups of the HBP and not solely with the OH groups of the VE. As a consequence, the T_g is reduced (cf. Fig. 3). However, when the OH functionality of the modifier is negligible, as for the six-arm star polymers 23V15 and

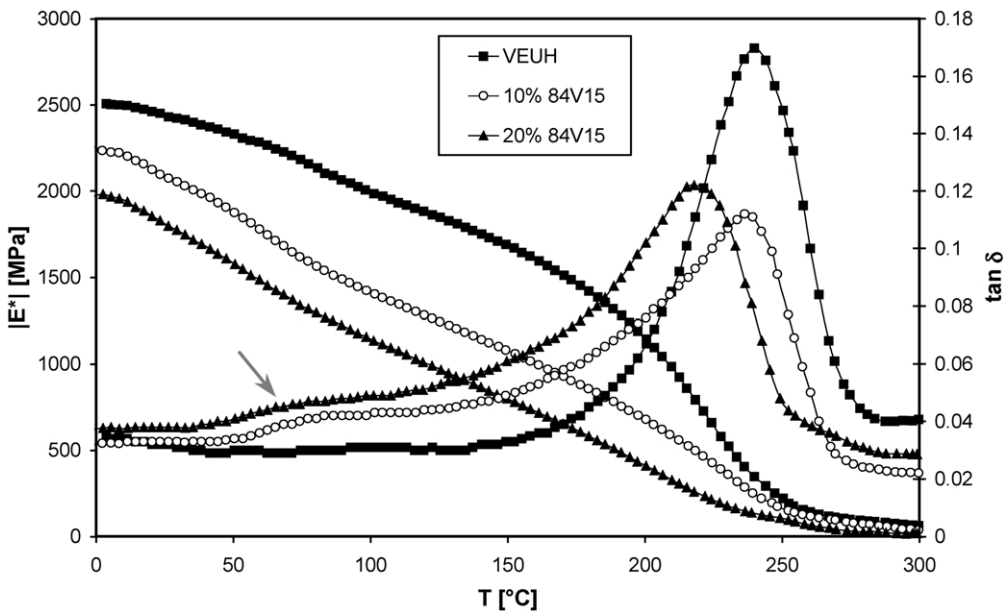

Fig. 3. $|E^*|$ vs. T and tan δ vs. T traces for VEUH without and with 10 and 20 wt% 84V15. For note cf. Fig. 1.

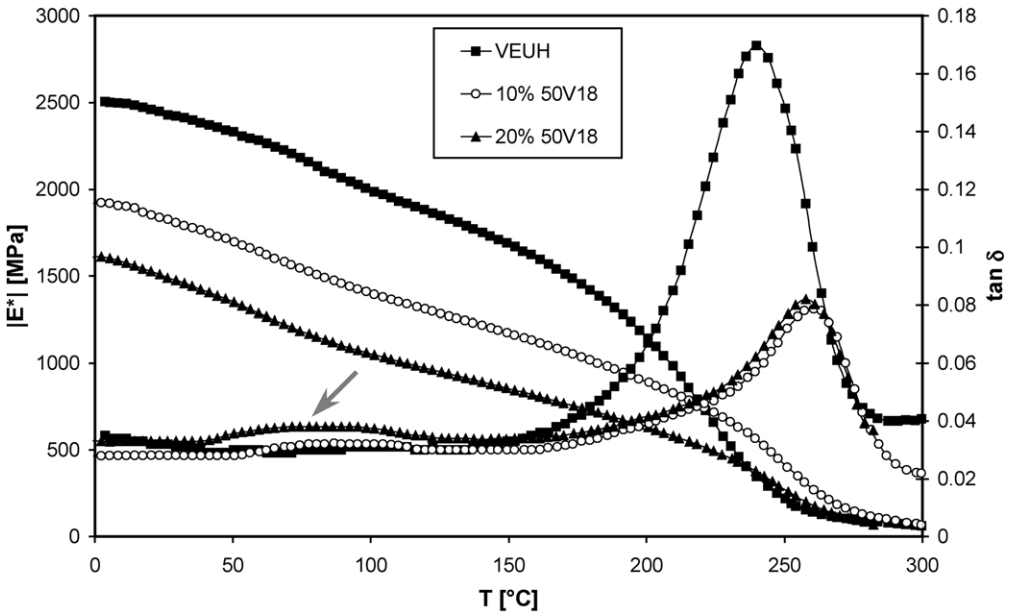

Fig. 4. $|E^*|$ vs. T and tan δ vs. T traces for VEUH without and with 10 and 20 wt% 50V18. For note cf. Fig. 1.

50V18, the isocyanate compounds react preferentially with the secondary hydroxy groups of the VE. This results in a tightly crosslinked network in which the inherent VE nodules change their shape due to the above cross reactions. This was shown by an AFM study performed on 'physically etched' specimens, recently [18]. Due to the cross reactions caused stress constraint the segmental mobility is restricted which is reflected by an elevated T_g (cf. Fig. 4).

3.4. Fracture mechanical response

Fig. 9 shows the fracture energy (G_c) of the HBP-modified VEUH resins. Comparing the G_c data, especially at 10 wt% modification, a strong effect of the type of the modifier can be recognized. The highest toughness improvement (almost four times higher than that of the neat VEUH) was found for 23V15 and 50V18 when added

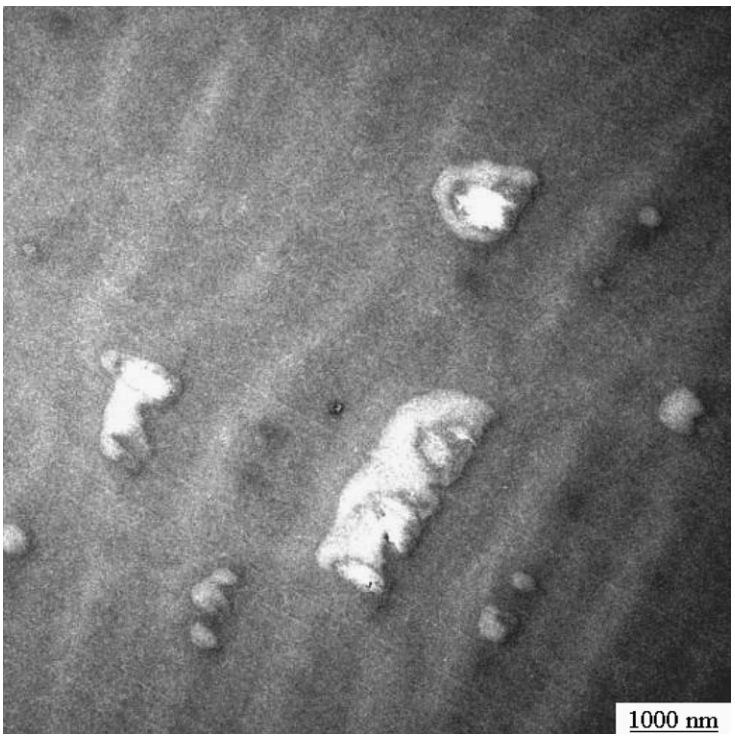

Fig. 5. TEM image taken from the VEUH modified by 20 wt% 25V10.

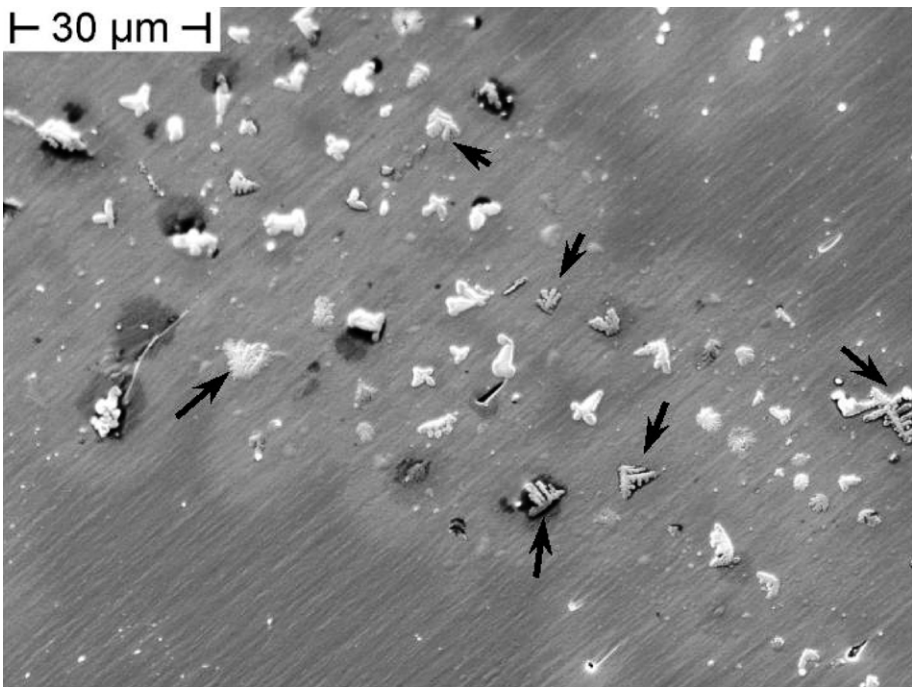

Fig. 6. SEM picture taken from the fast fracture range of VEUH containing 20 wt% 25V10.

at 10 wt%. Their increasing concentration yielded only a marginal increase in G_c. Recall that both of these six-arm star polymers showed type 3 DMTA response and a decrease in stiffness is usually accompanied by a toughness increase. The long flexible arms of these polymers guaranteed a more complete conversion of their vinyl groups compared to other HBP versions. Significant toughness enhancement with HBPs grouped into type 1 and 2 DMTA responses was achieved only when added at 20 wt%. Note that even at such high HBP loading, the G_c values of the VEUH modified with 10 wt% of 23V15 and 50V18 (type 3) were not reached. Nevertheless, the above findings already suggests that the G_c depends on the morphology.

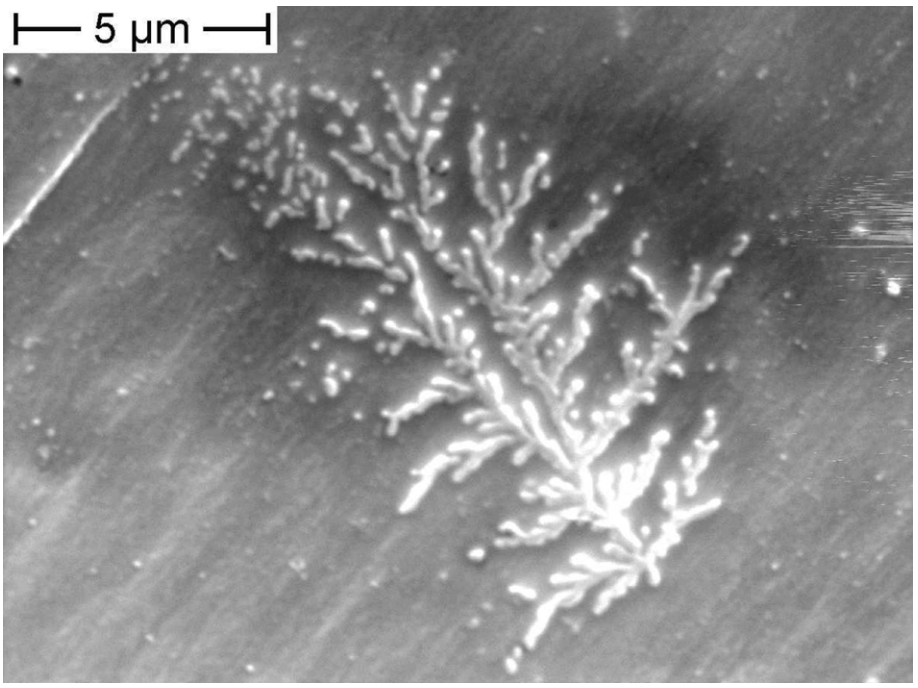

Fig. 7. SEM picture taken from the fast fracture range of VEUH containing 20 wt% 75V17.

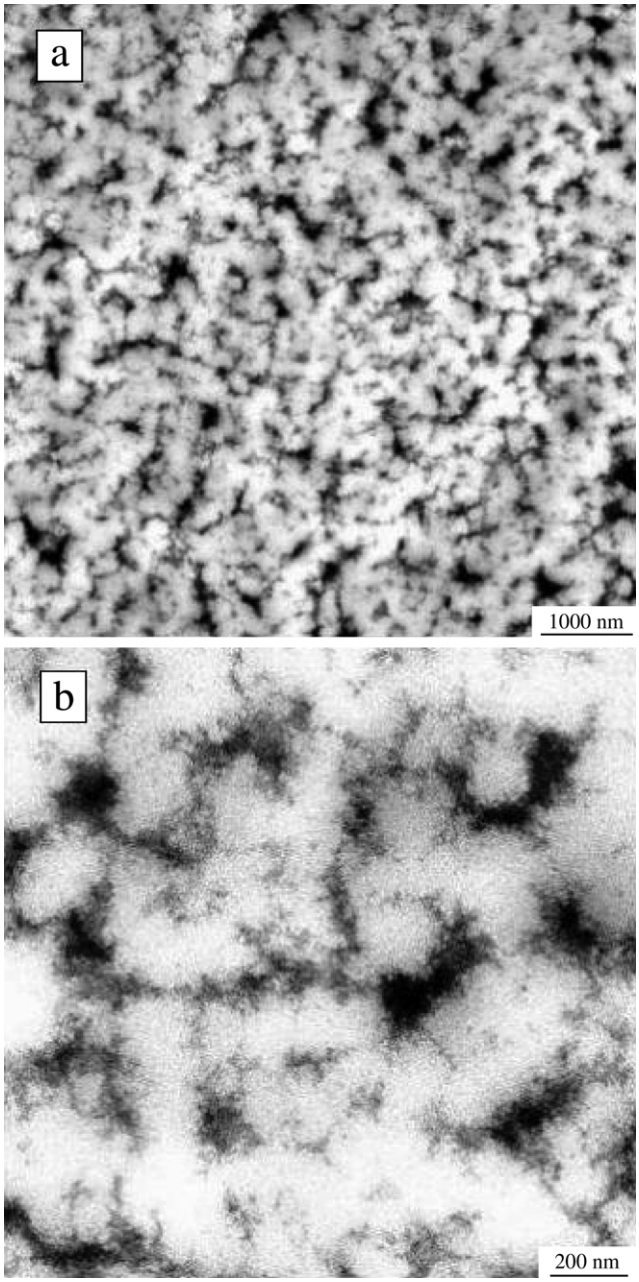

Fig. 8. TEM images at various magnifications from the VEUH containing 20 wt% 50V18.

3.5. Fractography

Modification of VEUH by HBPs enhances the shear deformability of the resin owing to the network inhomogeneities generated (cf. Figs. 10 and 11). Note that shear deformation is the major energy absorbing mechanism in thermosets which does not take place in VEUH [11]. Shear steps, termed river lines, are discernible on the SEM pictures in Fig. 10. Comparing the fracture surfaces in Fig. 10(a) and (b), one can claim that the shear deformability of the resin increases with decreasing stiffness. Thus the fracture energy is higher for the system toughened by type 2 modifier than by type 1. The scenario is similar for the VEUH modified by the six-arm star polymers showing type 3 DMTA response—cf. Fig. 11. The onset of prominent shear steps is obvious in Fig. 11(a). However, the highly magnified SEM picture shows a very rough fracture plane (cf. Fig. 11(b)). Recall that the fracture plane between the river lines was smooth in the systems showing lower G_c values (cf. Fig. 10). Thus, the outstanding fracture energy of the VEUH modified with star-like polymers showing type 3 DMTA response can be traced back to the formation of a quite regular, uniform network. Network regularity means that the segment lengths between the crosslinks are similar. This can be explained by supposing that in the copolymerization reactions the vinyl functionalities of VE, St and six-arm star polymer participate and polyaddition occurs mostly between the VE(–OH) and polyisocyanate. Further, the segregated phase during crosslinking is finely dispersed and eventual present in quasicontinuous form (IPN-like structure; cf. Fig. 8) which, being under constraint, may be responsible for the observed T_g shift. It is worth of noting that that both VE and VEUH show a nodular structure (i.e. phase-segregated) in nanometer scale [18]. The above explanation is in line with the DMTA results (i.e. appearance of a secondary relaxation at $T = 70\,^{\circ}C$ and a shift of the primary one toward higher T values in the related $\tan\delta$ vs T traces — cf. Fig. 4). Recall that the secondary transition appears as a peak for type 3 modifier instead of a shoulder as observed for HBPs of types 1 and 2 (cf. Figs. 2–4). A regular network structure favors the development of shear deformation which may occur in a diffuse manner (i.e. by multiple shear banding) — cf. Fig. 11.

4. Conclusions

Based on this work devoted to study the toughening effect of hyperbranched polyethers (HBP) and star polymers with various characteristics in a vinylester–urethane hybrid (VEUH) resin, the following conclusions can be drawn:

- Incorporation of branched polymers of various architectures and vinyl/hydroxy ratios strongly influenced the network formation and thus the resulting morphology. Compact HBPs with similar vinyl and hydroxy functionalities are not only involved in the copolymerization (with vinylester (VE) and styrene) and polyaddition reactions (with polyisocyanate) but also tend to homopolymerization by their C=C functionalities. The latter results in phase segregated inclusions.

- Less compact six-arm star polymers with high vinyl and negligible hydroxy functionalities copolymerize with VE and St and allow the polyaddition reactions to occur between VE and the polyisocyanate. The result is a complex morphology, however, with a quite regular crosslinked network structure. This phase structure causing stiffness reduction and Tg increase is more prone for diffuse shear

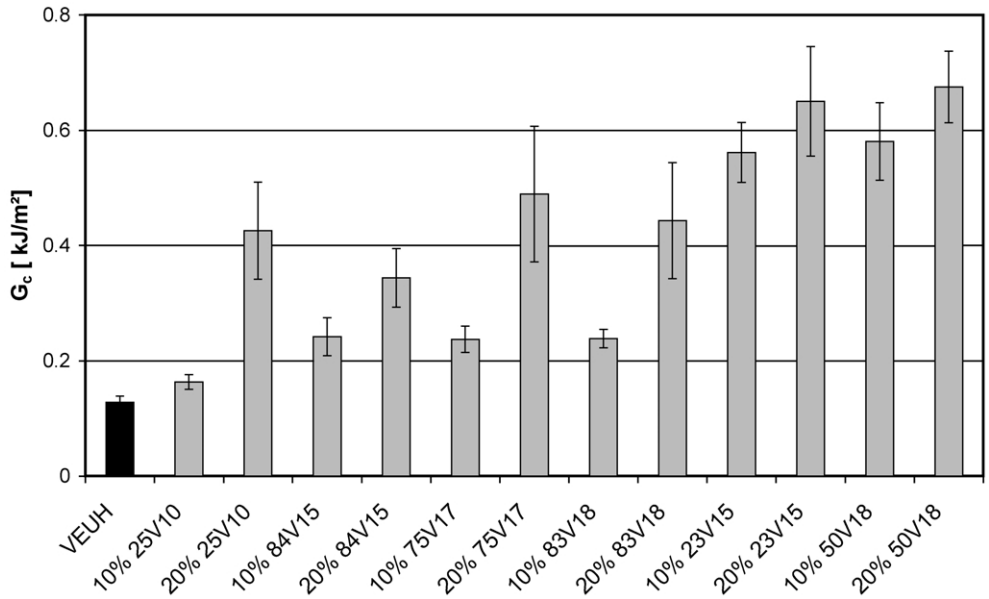

Fig. 9. Fracture energy (G_c) as a function of type and content of the toughness modifier used.

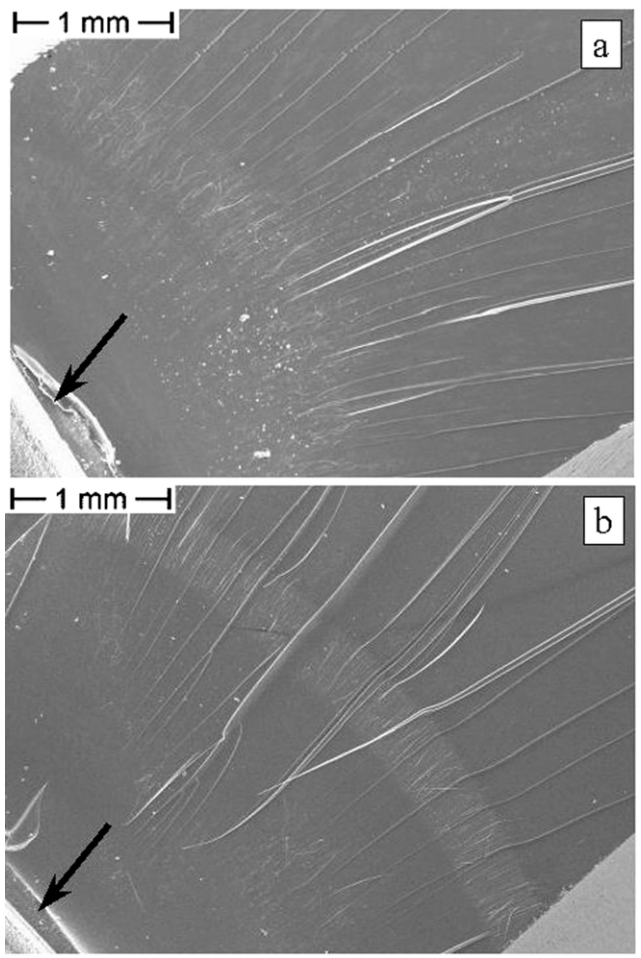

Fig. 10. SEM pictures taken from the fracture surface of VEUH modified by 10 wt% 25V10 (a) and 10 wt% 84V15 (b). Notes: the white spots are due to the homopolymerized HBP inclusions; arrow shows the razor blade notch.

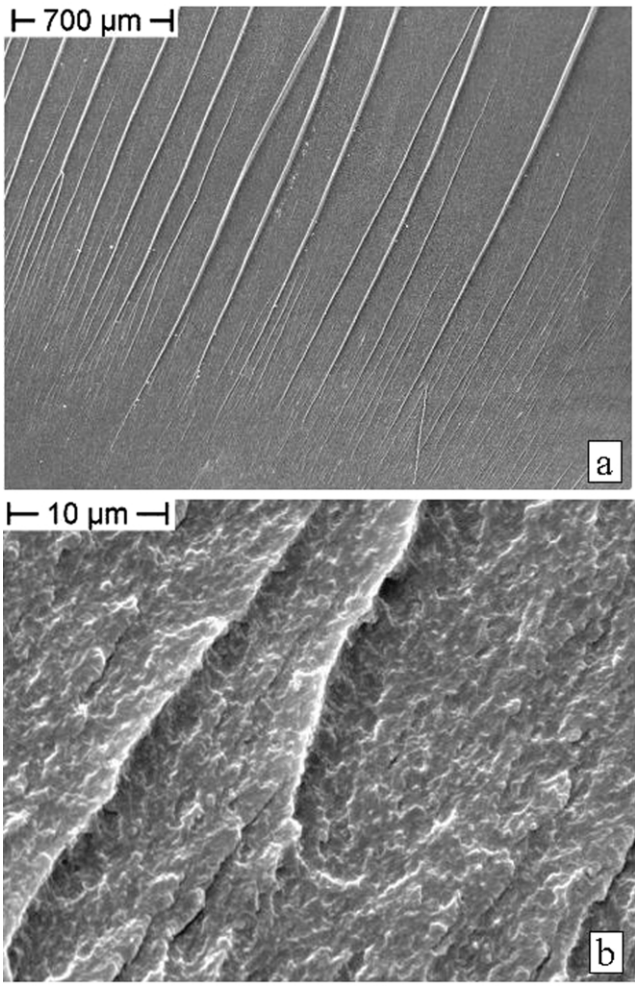

Fig. 11. SEM pictures at various magnifications taken from the fracture surface of VEUH modified by 10 wt% 50V18.

deformation. This kind of star polymer is the most efficient toughener in VEUH (the fracture energy of the plain VEUH can be quadrupled by adding 10 wt% of this functional polymer).

Acknowledgements

The authors wish to thank the German Science Foundation for the financial support of this project (DFG FOR 360; Ka 1202/9 and Mü 836/4). H. F. and H. K. thankfully acknowledge financial support and fellowships from the Fonds der Chemischen Industrie. We also acknowledge DSM Composite Resins (The Netherlands), Akzo Nobel Chemicals (Germany) and Bayer AG (Germany) for providing us with material samples.

References

[1] Tomalia DA, Frechet JM. J Polym Sci A: Polym Chem 2001;40:2719.
[2] Kim YH. J Polym Sci A: Polym Chem 1998;36:1685.
[3] Jannerfeldt G, Boogh L, Månson J-AE. Polymer 2000;41:7627.
[4] Voit B, Beyerlein D, Eichhorn K-J, Grundke K, Schmaljohann D, Loontjens T. Chem Engng Technol 2002;25:704.
[5] Mezzenga R, Pettersson B, Månson J-AE. Polym Bull 2001;46:419.
[6] Mezzenga R, Boogh L, Månson JA. Compos Sci Technol 2001;5:787.
[7] Mezzenga R, Plummer CJ, Boogh L, Månson JA. Polymer 2001;42:305.
[8] Gryshchuk O, Jost N, Karger-Kocsis J. Polymer 2002;43:4763.
[9] Eom Y, Boogh L, Michaud V, Månson J-A. Polym Compos 2002;23:1044.
[10] Jost N, Karger-Kocsis J. Polymer 2002;43:1383.
[11] Gryshchuk O, Jost N, Karger-Kocsis J. J Appl Polym Sci 2002;84:672.
[12] Sunder A, Hanselmann R, Frey H, Mülhaupt R. Macromolecules 1999;32:4240.
[13] Sunder A, Mülhaupt R, Frey H. Macromolecules 2000;33:309.
[14] Kautz H, Sunder A, Frey H. Macromol Symp 2001;163:67.
[15] Sunder A, Turk H, Haag R, Frey H. Macromolecules 2000;33:7682.
[16] Williams JG. In: Moore DR, Pavan A, Williams JG, editors. Fracture mechanics testing methods for polymers adhesives and composites. ESIS Publ 28. Oxford: Elsevier; 2001. p. 11.
[17] Karger-Kocsis J, Gryshchuk O. Macromol Symp 2004 (in press).
[18] Karger-Kocsis J, Gryshchuk O, Schmitt S. J Mater Sci 2003;38:413.